

## $\Sigma^0$ identification in proton induced reactions on a nuclear target<sup>†</sup>

---

**Tobias Kunz for the HADES Collaboration<sup>‡</sup>**

*Technische Universität München Fakultät für Physik, E62*

*Excellence Cluster Universe, Technische Universität München*

*E-mail: [tobias.kunz@tum.de](mailto:tobias.kunz@tum.de)*

We have studied the production of neutral  $\Sigma^0$  baryons in the reaction  $p+\text{Nb}$  at an incident proton energy of  $E_{\text{kin}} = 3.5$  GeV. The measurement has been performed with the HADES spectrometer at GSI, Darmstadt.  $\Sigma^0 \rightarrow \Lambda^0 \gamma$  and  $\Sigma^0 \rightarrow \Lambda e^+ e^-$  decays were identified via the charged decay  $\Lambda \rightarrow p \pi^-$  coincident to  $e^+ e^-$  pairs from external or internal gamma conversion. A total of net 220  $\Sigma^0$  candidates has been extracted. We present here the analysis method and the signal verification in simulations.

*The 55th Bormio Wintermeeting on Nuclear Physics*

*23-28 January, 2017*

*Bormio, Italy*

---

<sup>†</sup>Supported by BMBF (05P15WOFCA) and the DFG cluster of excellence 'Origin and Structure of the Universe'

<sup>‡</sup>Speaker.

## 1. Introduction

The properties of strange hadrons, i.e. baryons and mesons containing strange quarks, and their interaction with nucleons might undergo modifications within dense nuclear matter. The study of those effects in the energy regime of a few GeV close to the production threshold of light hyperons is found to be extremely favourable. At such energies dense baryonic matter can be produced in heavy ion collisions such that the study of strange hadron production under extreme conditions becomes accessible. Proton-induced reactions are then necessary as a reference case for understanding details of the production mechanism. Due to strangeness conservation, hyperon production has to be accompanied by the production of at least one kaon and hence leads to an energy threshold in NN of 2.518 GeV for  $\Lambda$  and 2.623 GeV for  $\Sigma^0$ . Plenty of data are available for  $\Lambda$  hyperons within a broad range of collision energies [1, 2, 3, 4, 5], while the situation is much more difficult for the  $\Sigma^0$  hyperon, where no data exists between 80 MeV and 2 GeV in excess energy above free nucleon nucleon production threshold [6, 7, 8].

An alternative method to study the hyperon-nucleon interaction is the spectroscopy of hypernuclei, i.e. nuclei where a hyperon replaces one of the nucleons. So far many  $\Lambda$ -hypernuclei have been measured in experiments with kaon beams [9, 10, 11] and in relativistic heavy ion collisions [12, 13, 14]. For the latter case, anti-hypertritons have been identified by the STAR collaboration in Au + Au collisions [15] at an energy of  $\sqrt{s_{NN}} = 200$  GeV [16]. Though, no evidence of  $\Sigma^0$  hypernuclei has been found so far.  $\Sigma^0$  undergo electromagnetic decays via  $\Sigma^0 \rightarrow \Lambda + \gamma$  (BR  $\approx$  100%) and hence are rather difficult to measure. On the other hand, the  $\Sigma$ -N interaction is barely known [17, 18] and it is not sure that  $\Sigma^0$ -hypernuclei can be formed at all. This lack of knowledge motivates further studies of the  $\Sigma^0$  production.

Only few experiments with p+p collisions either close to the production threshold [6, 7] or at an excess energy of around 5 GeV [8] have been successful in the measurement of  $\Sigma^0$  and  $\Lambda$  hyperons at the same time. So far, no data have been collected for proton + nucleus collisions in the regime of a few GeV excess energy. In this work we present the first analysis of  $\Sigma^0$  in p + Nb collisions at an incident beam energy of  $E = 3.5$  GeV as measured by the HADES collaboration.

## 2. The HADES spectrometer

The High Acceptance DiElectron Spectrometer (HADES) is located at the SIS18 accelerator at the Helmholtzzentrum für Schwerionenforschung (GSI) in Darmstadt. It covers the full azimuthal angle range and polar angles from  $18^\circ$  to  $85^\circ$  by using six identical sectors equipped with different detector types. Particle tracking and identification via  $dE/dx$  is performed with two layers of six Multiwire Drift Chambers (MDC) before and after a superconducting toroidal magnet. Electron and positron identification is realized by a Ring Imaging Cherenkov detector (RICH) with a Cherenkov threshold  $\gamma \simeq 18$  and an MWPC photon detector. In the present experiment, data has been collected with a proton beam of  $E_p = 3.5$  GeV incident energy on a twelve-fold segmented  $^{93}\text{Nb}$  target with a beam intensity of  $\approx 2 \cdot 10^6$  particles/s. The nuclear interaction probability for this target was 2.8%. The LVL1 trigger was set to a minimum multiplicity of three charged particle hits (M3) in both TOF walls. In total,  $3.2 \cdot 10^9$  events have been collected.

### 3. $\Lambda$ and photon reconstruction

The data sample has been analyzed with respect to a  $\Sigma^0 \rightarrow \Lambda + \gamma$  and  $\Sigma^0 \rightarrow \Lambda + e^+e^-$  decay signature. The identification of  $\Lambda$  candidates has been performed using the decay  $\Lambda \rightarrow p\pi^-$  (BR =  $(63.9 \pm 0.5) \%$  [19]) and the results for inclusive Lambda production in p+Nb reactions previously published by the HADES collaboration [20]. Due to the absence of an electromagnetic calorimeter, the decay photons were identified via their internal ( $\Sigma^0 \rightarrow \Lambda e^+e^-$ ) and external ( $\Sigma^0 \rightarrow \Lambda\gamma \rightarrow \Lambda e^+e^-$ ) pair conversion. The small  $\Sigma^0/\Lambda$  mass difference results in a comparatively small photon energy of  $E_\gamma = 77$  MeV and therefore to low energy electrons after conversion. In most of the cases, both conversion products could not be fully reconstructed, since the magnet  $B\rho \approx 0.3\text{Tm}$  setting in HADES resulted in an acceptance cut for low momentum electrons  $p_e \leq 50\text{-}80$  MeV/c. Nevertheless, even low momentum electrons leave a so-called tracklet signal in the two inner MDC tracking stations (MDCI and MDCII) in front of the B-field and produce a ring in the RICH detector, provided they overcome the Cherenkov threshold ( $\approx 15$  MeV/c). A schematic view of the  $\Sigma^0$  decay pattern is depicted in fig.1. All LVL1 trigger events with a track multiplicity

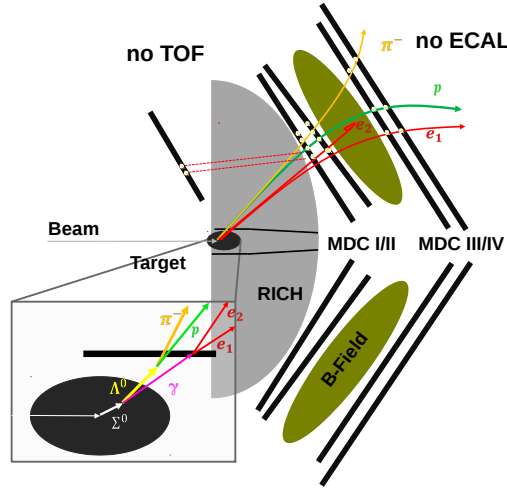


**Figure 1:** Schematic view of the  $\Sigma^0$  decay pattern within HADES. The  $\Sigma^0$  (white) decays inside the target region (box) into  $\Lambda$  (yellow)  $\gamma$  (magenta). The  $\Lambda$  decays into  $p$  (green) +  $\pi^-$  (orange) are fully reconstructed. The  $\gamma$  converts into an  $e^+/e^-$  (red) pair with one of the leptons not fully reconstructed due to strong bending in the magnetic field.

$3 < M < 7$  and a primary vertex reconstructed inside the target region ( $-3 \text{ mm} < x_{\text{VERTEX}} < 7 \text{ mm}$ ,  $-5 \text{ mm} < y_{\text{VERTEX}} < 5 \text{ mm}$ ,  $-65 \text{ mm} < z_{\text{VERTEX}} < 3 \text{ mm}$ ) were selected in our analysis.

To obtain the  $\Lambda$  signal, protons and pions were identified via their energy deposit in the MDC and TOF detector systems. The selection cuts have been chosen identical to the ones used in ref. [20]. Nominal mass values  $m_p = 938.272 \text{ MeV}/c^2$  and  $m_{\pi^-} = 139.570 \text{ MeV}/c^2$  [19] were then attributed to the identified particle candidates. For each proton-pion pair a secondary decay vertex was reconstructed applying cut criteria for the following topological variables: i) the distance between the primary and secondary vertex (VDX), ii) distances of the proton and pion tracks from the primary

vertex (VDp and VD $\pi$ ), iii) the distance between the proton and pion tracks (MTD) and iv) the opening angle between the tracks (oA) [20]. For the present analysis the cut criteria were chosen to be VDX > 35 mm, VDp < 6 mm, VD $\pi$  < 3 mm, MTD < 20 mm. Additionally, the opening angle was required to be oA > 4°. The obtained signal peak was subjected to a double gaussian fit resulting in a pole mass and width of  $m_\Lambda = 1115.4 \pm 0.2 \text{ MeV}/c^2$ ,  $\sigma_\Lambda = 3.3 \pm 0.1$  respectively, with a signal to background ratio S/B = 0.73 in a  $\pm 2\sigma$  window around the pole mass. The background was estimated with a polynomial function fitted to the invariant mass area outside the signal band. Background subtraction then yields a total of 1.35 million reconstructed  $\Lambda$ s.

Photons coincident to found  $\Lambda$  candidates were identified by a double ring signal in the RICH detector from both  $e^\pm$  conversion partners together with a fully reconstructed lepton track T and an incomplete lepton tracklet  $\tau$ . Since the number of detected Cherenkov photons is proportional to the track path length in the radiator, only conversion vertices in or close to the target are expected to contribute with the given photon detector efficiency. Simulations show that the expected conversion probability in the selected target region amounts to about 3%. The quality parameters of Cherenkov ring patterns in the photon detector govern the  $e^\pm$  identification efficiency and signal purity. In this analysis we have used cuts on the ring quality as described in ref. [21]. Correlated tracks and tracklets were required to geometrically match with a RICH ring center within an angle of ( $2.8^\circ < \Delta\theta < 8^\circ$ ). The lower limit of the matching window is due to the ring center position resolution as given by the RICH ring finder algorithm.

The momenta of  $e^\pm$  candidates are subject to two detection limits. In order to overcome the Cherenkov threshold  $\gamma \simeq 18$ , each of the two leptons needs a minimum energy  $E_{e^\pm} > 15 \text{ MeV}$ . The second detection limit is due to the acceptance cutoff of the given magnetic field strength. Dielectrons stemming from conversion processes of 80 MeV photons show similar kinematics as those from internal pair conversion in  $\pi^0$  Dalitz decays ( $\pi^0 \rightarrow e^+e^-\gamma$ ). For this reason, we have used the experimental results for  $\pi^0$  production in the p+Nb system to evaluate the detection limit for fully reconstructed low momentum electron tracks (T) as a function of polar angle. This limit varies from  $p \simeq 40 \text{ MeV}/c$  at a polar angle of  $85^\circ$  to  $p \simeq 100 \text{ MeV}/c$  at  $15^\circ$ . Hence, fully reconstructed tracks in the region of large polar angles will have a minimum momentum of 65 MeV/c.

The momentum of a lepton tracklet ( $\tau$ ) in an incompletely reconstructed pair has been calculated with the help of an event hypothesis (EH) method. For this purpose, a  $\Sigma \rightarrow \Lambda\gamma$  decay has first been simulated with the Pluto event generator [22] to extract a probability distribution for the tracklet momentum as a function of the T- $\tau$  opening angle and the track kinematic variables (momentum and angle). Then for each T- $\tau$  pair the momentum of the lepton tracklet was drawn according to this probability distribution.

The left panel of fig.2 shows the  $p\pi^-$  invariant mass distribution with a correlated T- $\tau$  photon conversion pair candidate in the same event. On top of a continuous background a  $\Lambda$  signal peak remains with a pole mass of  $m_\Lambda = 1114 \pm 2 \text{ MeV}/c^2$  and a width of  $\sigma_\Lambda = 2.23 \pm 0.16 \text{ MeV}/c^2$ .

To cross-check the validity of the photon reconstruction approach, a full scale Monte Carlo simulation was carried out for all p+Nb reaction products using the UrQMD transport code [23][24] and processing the events through the full HADES signal generation and analysis chain. In order to achieve sufficient event statistics, the UrQMD content of  $\Sigma$  hyperons was enhanced by a factor

60 while all other  $\gamma$  sources were kept at their default values. The right panel in fig.3 shows the reconstructed photon energy ( $E_\gamma$ ) distributions for the full scale simulation and the experiment data together with the PLUTO simulation input. The reconstructed photon energy peaks in all cases around 80 MeV and hence demonstrates the validity of the applied procedure. The reconstructed signal has been fitted using a convolution of an exponential and a gaussian function. A FWHM of  $57 \pm 2$  for the experimental data and  $53 \pm 2$  for the simulation has been obtained.

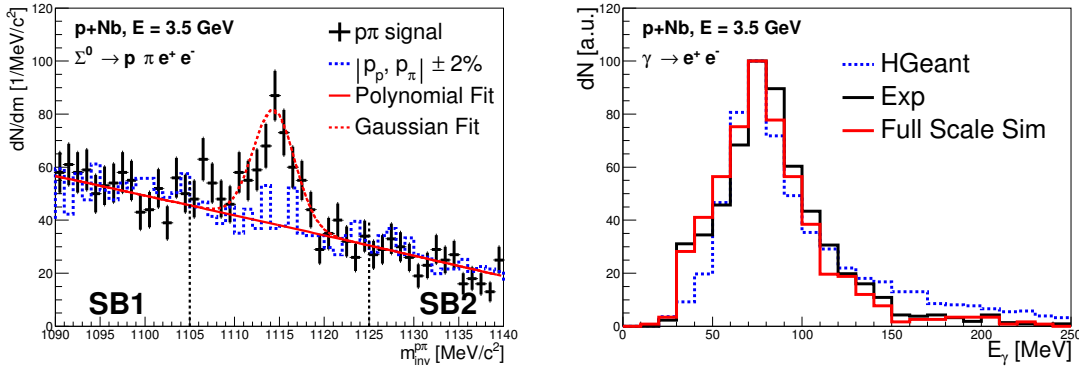


**Figure 2:** *Left:* Invariant mass distribution of  $p\pi$ -pairs with an additional  $e^\pm$  pair in the same event. A polynomial fit (red) and momentum smeared pairs (blue) describe the background similarly well. *Right:* Energy distribution of the reconstructed  $e+e^-$  conversion pair in comparison to the simulation input (blue, “HGeant”) and the full scale simulation reconstruction result (red, “Sim”).

#### 4. Background subtraction and $\Sigma^0$ signal

The signal region in the  $p\pi$  invariant mass distribution is confined to a window  $1105 \text{ MeV}/c^2 < m_{p\pi}^{\text{inv}} < 1125 \text{ MeV}/c^2$ . The background inside this window has been extracted utilizing two different methods. Two sideband intervals have been defined in the  $p\pi^-$  invariant mass  $1090 \text{ MeV}/c^2 < m_{p\pi}^{\text{inv}} < 1105 \text{ MeV}/c^2$  (SB1) and  $1125 \text{ MeV}/c^2 < m_{p\pi}^{\text{inv}} < 1140 \text{ MeV}/c^2$  (SB2). In a first approach, a polynomial fit of the invariant mass distribution in the sideband windows has been extrapolated to the signal region. In the second approach, a background sample with realistic kinematic observables like transverse momenta of  $p\pi^-$  pairs has been applied. This sample has been constructed by artificially smearing the pair constituent momenta of identified  $\Lambda$  candidates by  $\pm 2\%$ . Figure 3 shows the comparison of the corresponding pair- $p_t$  distributions obtained for the unsmeared sideband samples SB1 and SB2 (dashed and full line, respectively) with the one for the momentum smeared signal pairs. The effective background strength in the signal band was then adjusted to the weighted sum of the SB1 and SB2  $p_t$  distribution yields.

Combining  $\Lambda$  signal events with reconstructed  $e^\pm$  pairs yields the experimental four particle ( $p\pi e^\pm$ ) invariant mass distribution as depicted in fig.3. A peak structure close to the nominal  $\Sigma^0$  mass ( $m_{\Sigma^0} = 1192 \text{ MeV}/c^2$  [19]) emerges. The available phase space and the kinematic observables for the  $\Sigma^0$  and  $\Lambda^0$  hyperons are expected to be very similar, due to their comparable masses. In the present analysis we assume that the same holds true also for background  $p\pi^-$  pairs from other sources. Hence, the corresponding sidebands in the four particle ( $p\pi e^\pm$ ) invariant mass distribution are dominated by  $p\pi$  pairs from the  $\Lambda$  spectrum. Sideband contributions resulting from the finite

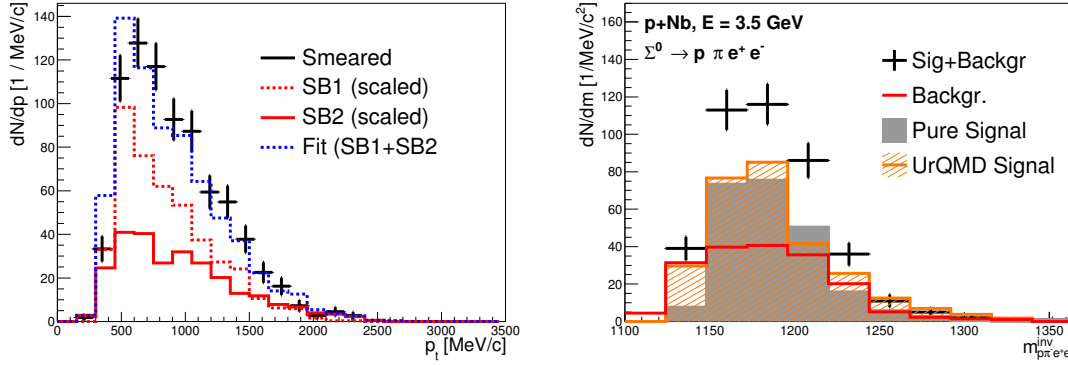


**Figure 3:** Left panel:  $p_t$  distributions of SB1, SB2 and the smeared signal region for  $p\text{-}\pi$  pairs. A combination of SB1 and SB2 is fitted to the smeared signal region to mimic the background and is shown in blue. Right panel: Four particle invariant mass distribution of combined  $p\pi^-$  and dielectron pairs. The extracted signal from a full scale UrQMD simulation with properly scaled  $\Sigma^0$  content is shown for comparison.

resolution of the  $\gamma$  reconstruction are expected to be negligible. Consequently, and in analogy to the  $\Lambda$  sidebands, the four particle background BG is then given by  $BG = a \cdot SB1^\Sigma + b \cdot SB2^\Sigma$  with the same parameters  $a = 0.38$  and  $b = 0.55$  as determined above. The net  $\Sigma^0$  signal obtained after background subtraction is shown as gray histogram in fig.3 (right panel) and yields 220 counts. The simulated  $\Sigma^0$  distribution obtained from properly scaled UrQMD simulations shows a reasonable agreement obtained between the experimental and simulated distributions.

## 5. Summary

We presented the analysis procedure applied to extract a  $\Sigma^0$  hyperon signal in p+Nb collisions at a beam energy  $E_{kin} = 3.5$  GeV. Utilizing the identification and momentum reconstruction of four charged particles emerging from the decay chain  $\Sigma^0 \rightarrow \Lambda\gamma \rightarrow p\pi^- + e^+e^-$  we observe a total of around 220 net  $\Sigma^0$  counts in a sample of  $3.2 \cdot 10^9$  recorded events. The  $\gamma$  energy determination is shown to be feasible even for conversion pairs with a missing charge and momentum measurement for one  $e^\pm$  partner. The background has been determined with a sideband technique and is small. In a future analysis we will extract differential cross sections and compare them to world data in different energy domains as well as to predictions from transport model codes and statistical models.

## Acknowledgements

The HADES Collaboration gratefully acknowledges the support by BMBF grants 06DR9059D, 05P12CRGHE, 06FY171, 06MT238 T5, and 06MT9156 TP5, by HGFVH-NG-330, by DFG EClust153, by GSI TMKRUE, by the Hessian LOEWE initiative through HIC for FAIR (Germany), by EMMI GSI, TU Darmstadt (Germany): VH-NG-823, Helmholtz AllianceHA216/EMMI, by grant GA CR 13-067595 (Czech Rep.), by grant NN202198639 (Poland), Grant UCY/3411-23100 (Cyprus), by CNRS/IN2P3 (France), by INFN (Italy), and by EU contracts RII3-CT-2005-515876 and HP2 227431.

## References

- [1] COSY-TOF collaboration, S. Abdel-Samad et al., *Hyperon production in the channel  $p p \rightarrow K + \Lambda p$  near the reaction threshold*, *Phys. Lett.* **B632** (2006) 27–34.
- [2] COSY-TOF collaboration, M. Röder et al., *Final-State Interactions in the Process  $\bar{p}p \rightarrow pK^+\Lambda$* , *Eur. Phys. J.* **A49** (2013) 157, [1305.0451].
- [3] R. Siebert et al., *High resolution study of hyperon nucleon interactions by associated strangeness production in  $p p$  collisions*, *Nucl. Phys.* **A567** (1994) 819–843.
- [4] COSY-TOF collaboration, F. Hauenstein et al., *First Model-Independent Measurement of the Spin Triplet  $p\Lambda$  Scattering Length from Final State Interaction in the  $\bar{p}p \rightarrow pK^+\Lambda$  Reaction*, *Phys. Rev.* **C95** (2017) 034001, [1607.04783].
- [5] HADES collaboration, G. Agakishiev et al., *Baryonic resonances close to the  $\bar{K} N$  threshold: The Case of  $\Sigma(1385)^+$  in  $pp$  collisions*, *Phys. Rev.* **C85** (2012) 035203, [1109.6806].
- [6] S. Sewerin et al., *Comparison of lambda and sigma0 threshold production in proton proton collisions*, *Phys. Rev. Lett.* **83** (1999) 682–685, [nucl-ex/9811004].
- [7] P. Kowina et al., *Energy dependence of the Lambda / Sigma0 production cross-section ratio in  $p p$  interactions*, *Eur. Phys. J.* **A22** (2004) 293–299, [nucl-ex/0402008].
- [8] A. Baldini, *Numerical data and functional relationships in science and technology, Springer 409 P., Landolt-Boernstein, New Series 1/128* **12** (1988).
- [9] G. Keyes, J. Sacton, J. H. Wickens and M. M. Block, *Measurement of Decay Branching Ratios for the He-4 (Lambda) Hypernucleus*, *Nuovo Cim.* **A31** (1976) 401.
- [10] G. C. Bonazzola, T. Bressani, E. Chiavassa, G. Dellacasa, A. Fainberg, M. Gallio et al., *Observation of the Hypernuclei  $^{16}O$  and  $^{27}Al$* , *Phys. Rev. Lett.* **34** (1975) 683–686.
- [11] A. S. Mondal, A. K. Basak, M. M. Kasim and A. Husain, *A Probable Example of a Lambda C-14 Hypernucleus*, .
- [12] A. S. Botvina, K. K. Gudima, J. Steinheimer, M. Bleicher and J. Pochodzalla, *Formation of hypernuclei in heavy-ion collisions around the threshold energies*, *Phys. Rev.* **C95** (2017) 014902, [1608.05680].
- [13] J. Steinheimer, K. Gudima, A. Botvina, I. Mishustin, M. Bleicher and H. Stöcker, *Hypernuclei, dibaryon and antinuclei production in high energy heavy ion collisions: Thermal production versus Coalescence*, *Phys. Lett.* **B714** (2012) 85–91, [1203.2547].
- [14] ALICE collaboration, A. G. Knospe, *Resonances as Probes of Heavy-Ion Collisions at ALICE*, *J. Phys. Conf. Ser.* **612** (2015) 012064, [1501.03797].
- [15] N. Shah, Y. G. Ma, J. H. Chen and S. Zhang, *Production of multistrange hadrons, light nuclei and hypertriton in central Au+Au collisions at  $\sqrt{s_{NN}} = 11.5$  and 200 GeV*, *Phys. Lett.* **B754** (2016) 6–10, [1511.08266].
- [16] STAR collaboration, B. I. Abelev et al., *Observation of an Antimatter Hypernucleus*, *Science* **328** (2010) 58–62, [1003.2030].
- [17] H. Nemura et al., *Lambda-Nucleon and Sigma-Nucleon interactions from lattice QCD with physical masses*, *PoS LATTICE2016* (2017) 101, [1702.00734].

- [18] J. C. Helder and J. J. De Swart, *Low energy sigma-nucleon scattering*, *Conf. Proc.* **C690505** (1969) 842–851.
- [19] PARTICLE DATA GROUP collaboration, C. Patrignani et al., *Review of Particle Physics*, *Chin. Phys.* **C40** (2016) 100001.
- [20] HADES collaboration, G. Agakishiev et al., *Lambda hyperon production and polarization in collisions of  $p(3.5\text{ GeV})+Nb$* , *Eur. Phys. J.* **A50** (2014) 81, [1404.3014].
- [21] HADES collaboration, M. Weber et al., *Inclusive  $e^+e^-$  pair production in  $p+p$  and  $p+Nb$  collisions at  $E(\text{kin}) = 3.5\text{-GeV}$* , *J. Phys. Conf. Ser.* **316** (2011) 012007.
- [22] I. Fröhlich et al., *Pluto: A Monte Carlo Simulation Tool for Hadronic Physics*, *PoS ACAT2007* (2007) 076, [0708.2382].
- [23] S. A. Bass et al., *Microscopic models for ultrarelativistic heavy ion collisions*, *Prog. Part. Nucl. Phys.* **41** (1998) 255–369, [nucl-th/9803035].
- [24] M. Bleicher et al., *Relativistic hadron hadron collisions in the ultrarelativistic quantum molecular dynamics model*, *J. Phys.* **G25** (1999) 1859–1896, [hep-ph/9909407].